Inorganic Chemistry

ARTICLE

pubs.acs.org/IC

Bixbyite-Type V_2O_3—A Metastable Polymorph of Vanadium Sesquioxide

D. Weber,[†] A. Stork,[†] S. Nakhal,[†] C. Wessel,[‡] C. Reimann,[§] W. Hermes,[∥] A. Müller,[†] T. Ressler,[†] R. Pöttgen,[∥] T. Bredow,[§] R. Dronskowski,[‡] and M. Lerch*[,†]

[†]Institut für Chemie, TU Berlin, Strasse des 17. Juni 135, D-10623 Berlin, Germany

[‡]Institut für Anorganische Chemie, RWTH Aachen University, Landoltweg 1, D-52056 Aachen, Germany

[§]Institut für Physikalische und Theoretische Chemie, Universität Bonn, Wegelerstrasse 12, D-53115 Bonn, Germany

[∥]Institut für Anorganische und Analytische Chemie, Universität Münster, Corrensstrasse 30, D-48149 Münster, Germany

ABSTRACT: A metastable polymorph of vanadium sesquioxide was prepared by the reaction of vanadium trifluoride with a water-saturated gaseous mixture of 10 vol % hydrogen in argon. The new polymorph crystallizes in the bixbyite-type structure. At temperatures around 823 K a transformation to the well-known corundum-type phase is observed. Quantum-chemical calculations show that the bixbyite-type structure is about 9 kJ/mol less stable than the known corundum-based one. This result, in combination with the absence of imaginary modes in the phonon density of states, supports the classification of the bixbyite-type phase as a metastable V_2O_3 polymorph. At ~50 K a paramagnetic to canted antiferromagnetic transition is detected.

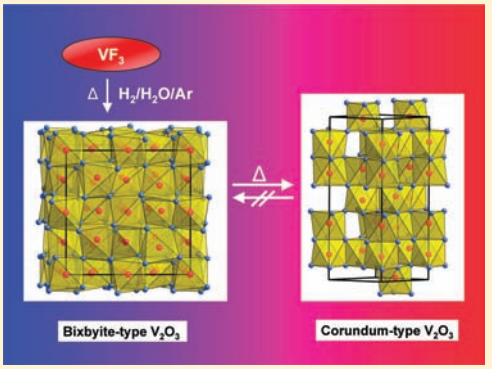

INTRODUCTION

Because of their physical and chemical properties, vanadium oxide-based materials have attracted broad attention in the last few decades. These compounds are used in various technical applications, for example, as catalysts,[1,2] chemical sensors,[3] cathode materials for high-density lithium batteries,[4] and in other electronic and optical devices.[5] In addition, binary vanadium oxides have been the subject of numerous investigations. As a prominent example, a lot of detailed studies were carried out on V_2O_3 due to the unique fact that a magnetic transition and a metal−insulator transition (often described as a Mott−Hubbard transition[6,7]) occur at the same temperature. At ambient temperature V_2O_3 crystallizes in the well-known rhombohedral corundum-type structure with a notably large c/a ratio of 2.823. It is paramagnetic and exhibits metallic behavior. Upon lowering the temperature, a structural phase transition to a monoclinic polymorph (M1 phase) occurs at around 170 K. This phase is antiferromagnetically ordered and an electric insulator.[7−11] To the best of our knowledge, no other vanadium sesquioxides exist. Keeping in mind the unique physical properties of the sesquioxide, preparation and characterization of an additional polymorph are of fundamental interest.

EXPERIMENTAL SECTION

All reactions were carried out in a conventional tube furnace equipped with a corundum tube with an inner diameter of 50 mm. The flow rate of the reaction gas (NOXAL4, Air Liquide, 10 ± 1 vol % H_2 in Ar, gas stream piped through a water-filled washing flask) was regulated with a needle valve and has been optimized to 10 $L \cdot h^{-1}$. VF_3 (200−500 mg; 98%, Apollo Scientific) was placed in a small alumina boat inside the tube and heated under flowing reaction gas for 2.5 h at 873 K. The hydrogen and water contents of the gas atmosphere are the main determinants of the oxygen activity in the furnace, which is the most important parameter controlling the reaction of VF_3 to V_2O_3 and avoiding oxidation or reduction of vanadium. Consequently, it must be emphasized that the reaction conditions must be optimized carefully. Otherwise, remaining fluorine, large amounts of the corundum-type phase, partial oxidation to vanadium dioxide, or significant deviations from the ideal V_2O_3 stoichiometry are observed. The products were characterized by X-ray powder diffraction (Siemens D5000 with Cu $K\alpha_1$ radiation, λ = 154.05 pm) and in-situ high-temperature XRD (STOE Stadi-P, graphite-heated furnace, samples in SiO_2-glass capillaries under dried argon) with Mo $K\alpha_1$ radiation (λ = 70.93 pm). The program packages Powder Cell 2.4[12] and FullProf July 2009[13] were used for structural refinements. Peak profiles were fitted with a Pseudo-Voigt function. Quantitative analysis of the oxygen content was performed by the well-established hot gas extraction method (LECO TC300/EF300). For this method selection of standards is of importance. For our measurements on bixbyite-type vanadium sesquioxides we chose zirconia and corundum-type V_2O_3, which is known for its small range of nonstoichiometry from room temperature to 900 K. The accuracy is ~2% of the presented oxygen

Received: April 19, 2011
Published: June 13, 2011

content ($V_2O_{3\pm0.06}$). Qualitative hydrogen and fluorine analyses were performed by ^{1}H-MAS NMR and ^{19}F-MAS NMR (Bruker Avance II), respectively. Additionally, the chemical composition was examined by quantitative X-ray fluorescence measurements (PANalytical Axios PW 4400/24, corundum-type V_2O_3 as internal standard), energy-dispersive X-ray spectroscopy (EDX, Hitachi S-2700), and elemental analysis (CHNS, ThermoFinnigan Flash EA 1112). No significant amounts of fluorine or hydrogen could be detected. Respecting the detection limits of the methods and equipment used, it can be stated that the amount of hydrogen is below 0.1 wt % and that of fluorine below 0.5 wt %. Thermoanalytical (DTA/TG) analysis (Linseis L81 II) was put into execution under 10 vol % hydrogen in argon (NOXAL4, Air Liquide, 80 mL·h^{-1}).

X-ray absorption spectroscopy (XAS) measurements were performed at the V K edge (5.465 keV, Si 111) at the Hamburg Synchrotron Radiation Laboratory, HASYLAB. The materials were mixed with polyethylene (~5 mg of oxide and ~30 mg of PE) and pressed to a pellet (13 mm diameter) with a force of 2 tons. For XAS data analysis background subtraction and normalization were carried out by fitting linear polynomials to the pre-edge and the post-edge region of the absorption spectra, respectively.[14] The pseudo-radial distribution function FT($\chi(k)k^3$) was calculated by Fourier transforming the k^3-weighted experimental χ (k) function (k range from 2.0 to 11.1 Å^{-1}), multiplied by a Bessel window, into the R space.

Physical Property Measurements. A 12.831 mg amount of the V_2O_3 powder sample was packed in a commercial VSM capsule and attached to the sample holder rod of a VSM for measuring the magnetic properties in a Quantum Design Physical-Property-Measurement-System in the temperature range 2.1−305 K with magnetic flux densities up to 80 kOe. For heat capacity (C_p) measurements (2.1−100 K) 10.385 mg of cold-pressed V_2O_3 was glued to the platform of a precalibrated heat capacity puck using Apiezon N grease.

Computational Details. Periodic density-functional calculations were performed with the crystalline orbital program CRYSTAL[15,16] and the plane-wave code VASP.[17] All DFT calculations were carried out within the generalized-gradient approximation, employing Perdew, Burke, and Ernzerhof (PBE-GGA)[18] and Perdew and Wang (PW-GGA)[19] exchange-correlation functionals. This computational setup has been successfully used in our previous studies of the Ta−O−N system.[20] VASP calculations were performed using the projector-augmented-wave (PAW) method[21] for the separation of core and valence electrons. Furthermore, the self-interaction correction and the electron−electron-Coulomb interaction were approximately treated by the rotationally invariant GGA+U approach according to Liechtenstein[22] with U = 2.8 eV and J = 0.93 eV, which have been successfully applied for V_2O_3.[23] The quasiharmonic phonons were calculated with the help of the program FROPHO.[24] To do so, all symmetry-inequivalent atoms of a supercell were slightly shifted off their equilibrium position. On the basis of the resulting Hellmann−Feynman forces the force constants were calculated, which consequently resulted in the dynamical matrix. Combining its eigenvalues (phonon frequencies) with Bose−Einstein statistics, thermodynamic properties at finite temperatures are straightforward.[25] In the CRYSTAL calculations, effective core potentials (ECP) were used for the vanadium atoms (SD10MDF[26]) for better comparability with the VASP PAW results. The validity of this approximation has been assessed by comparison with lattice properties calculated with previously published all-electron (AE) basis sets.[27] The Stuttgart/Cologne ECP basis sets[28] have been reoptimized in order to yield basis sets with well-defined degrees of freedom in the valence part that are suitable for solid-state calculations. Vanadium basis sets of valence double- and triple-ζ quality (VDZ and VTZ) were obtained that were further augmented with one polarization f shell (VDZP and VTZP). For oxygen, an optimized all-electron basis set of valence triple-ζ quality (AE-VTZP) was used in all calculations.[29]

RESULTS AND DISCUSSION

We were successful in the synthesis of a new polymorph of vanadium sesquioxide (for technical details see Experimental Section). The obtained grayish-black product was structurally characterized using X-ray powder diffraction. Although the optimized reaction conditions yielded a maximum phase fraction of more than 80 wt %, the new polymorph could not yet be isolated as a pure phase. The competing phase is always the well-known corundum-type V_2O_3. For lower hydrogen contents in the reaction gas formation of VO_2(M) is observed.

The new phase crystallizes in the bixbyite-type structure with the lattice parameter a = 939.47(2) pm in space group $Ia\bar{3}$ (no. 206). The results of the Rietveld refinement are given in Figure 1 and Tables 1 and 2. In principle, the bixbyite-type structure can be derived from the fluorite-type structure by removing 1/4 of the anions. The ordered arrangement of oxygen vacancies leads to a reduction of the symmetry with a doubling of the lattice parameters. Figure 2 (right) depicts the unit cell and roughly points out the relationship between fluorite and bixbyite type. The cations are located on 8a (0,0,0) and 24d (x,0,1/4) positions, while the anions occupy the general position 48e (x,y,z). All cations are octahedrally coordinated by six anions and the anions tetrahedrally by the cations. The VO_6 octahedra together with the bond lengths, which are in good agreement with expected values, are presented in Figure 3. The average bond length of 202.8 pm is slightly larger than that of corundum-type V_2O_3 (202.1 pm). Comparing the determined densities (Table 1) it is remarkable that the value of the bixbyite-type polymorph is ~4% smaller. Consequently, this phase cannot be prepared from the corundum-type polymorph by high-pressure methods.

The V K edge XANES spectra of corundum-type and bixbyite-type V_2O_3 are compared in Figure 4. The very similar pre-edge peak height in the spectra of both compounds indicates an average valence of 3 for bixbyite-type V_2O_3. A significant amount of V(IV) or V(V) species (>5%) can be excluded. The FT($\chi(k)k^3$) of bixbyite-type V_2O_3 is depicted together with that of corundum-type V_2O_3 in Figure 4. The pronounced amplitude at higher distances in the FT($\chi(k)k^3$) of bixbyite-type V_2O_3 is indicative of a well-ordered local structure together with a reduced distribution of distances according to the higher symmetry of bixbyite-type V_2O_3 compared to corundum-type V_2O_3. Moreover, the characteristic shape of the XANES spectra and the FT($\chi(k)k^3$) of bixbyite-type V_2O_3 are very similar to those of the previously reported bixbyite-type vanadium oxide nitride.[30] This corroborates the identification of the vanadium oxide as bixbyite-type V_2O_3.

As it is known from nitrides and oxide nitrides, for example, U_2N_3,[31,32] Zr_2ON_2,[33] or vanadium oxide nitrides,[30] anion vacancies in bixbyite-type compounds can be partially occupied by additional anions, resulting in compositions $A_2X_{3+\delta}$. In the ideal fluorite stoichiometry (AX_2) these anion vacancies are fully occupied. Quantitative oxygen analysis of the sample resulted in 32.1 wt % oxygen. Taking into account the oxygen content of the corundum-type V_2O_3 side phase, which is known to have no large deviation from the ideal stoichiometry at the temperature of synthesis, the resulting $V_2O_{3.01}$ composition is in good agreement with the ideal bixbyite stoichiometry. Again, it should be mentioned that the conditions of synthesis presented here have to be met carefully. Slightly different conditions result in bixbyite-type phases with significant deviations from the ideal V_2O_3 stoichiometry. This will be shown in a forthcoming contribution and

dx.doi.org/10.1021/ic200799n |Inorg. Chem. 2011, 50, 6762–6766

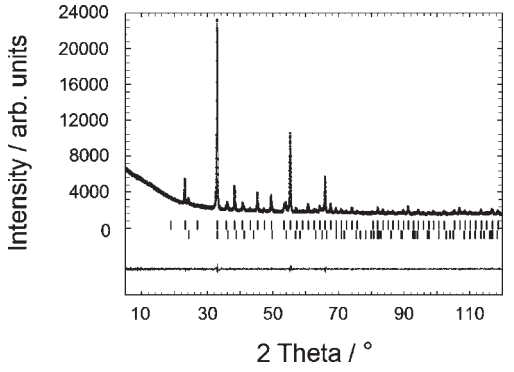

Figure 1. X-ray powder diffraction diagram of bixbyite-type V_2O_3 with the results of the Rietveld refinement. The Bragg reflection positions of the main phase (upper row) and corundum-type V_2O_3 are indicated.

Table 1. Results of the Rietveld Refinement

composition	V_2O_3	V_2O_3
structure type	bixbyite	corundum
space group	$Ia\bar{3}$	$R\bar{3}c$
lattice parameters	a = 939.47(1) pm	a = 496.23(2) pm
		c = 1398.4(1) pm
formula units	16	6
unit cell volume (normalized to one formula unit)	51.96 × 10^6 pm^3	49.88 × 10^6 pm^3
calculated density	4.79 g/cm^3	4.99 g/cm^3
phase fraction	82(1) wt %	18(1) wt %
diffractometer	Siemens D5000	
wavelength	Cu Kα_1 (λ = 154.056 pm)	
profile points	4540	
2θ range	5−120°	
R_{Bragg}	0.0056	0.0161
R_{wp}	0.0078	
R_{exp}	0.0073	
S	1.08	

Table 2. Refined Structural Parameters for Bixbyite-Type V_2O_3

atom	site	x	y	z	B_{iso}/Å^2
V1	8a	0	0	0	1.0(1)
V2	24d	0.2822(1)	0	1/4	1.34(9)
O1	48e	0.1424(5)	0.1316(6)	−0.0969(4)	1.3(1)

should not be discussed here. Chemical analyses of the material show neither significant amounts of incorporated hydrogen nor remaining fluorine (see Experimental Section for details).

The relative stability of selected vanadium sesquioxide polymorphs was studied theoretically at the density-functional theory (DFT) level. In order to investigate the effect of basis sets on structural and thermodynamical properties, complementary methods were employed in which the crystalline orbitals were expanded in either plane waves (PW) or atom-centered Gaussian functions (GTO). Lattice parameters and atomic positions were optimized for 6 hypothetical crystal structures with the

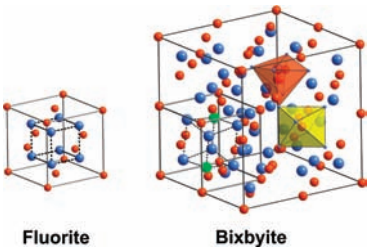

Figure 2. Relationship between fluorite- and bixbyite-type: (red) cation, (blue) anion. Two of the oxygen vacancies, completing the fluorite-type anion cube, are shown exemplarily (green). Selected coordination polyhedra around V1 (yellow) and V2 (orange) are depicted.

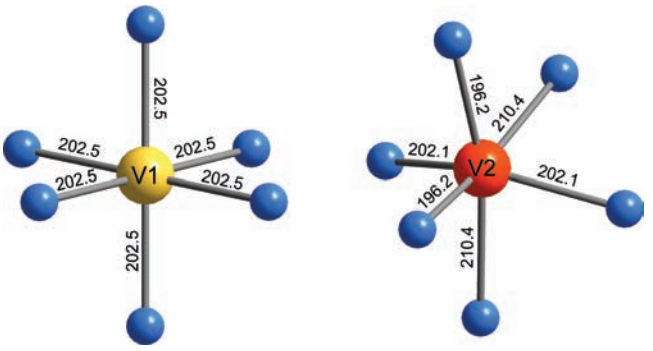

Figure 3. Coordination polyhedra and bond lengths in bixbyite-type V_2O_3.

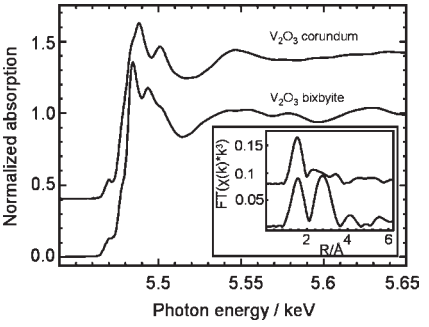

Figure 4. V K edge XANES spectra and FT($\chi(k)k^3$) (inset) of corundum-type and bixbyite-type V_2O_3 (corresponding to 82% V_2O_3 bixbyite).

composition V_2O_3. In agreement with experiment the low-temperature M1 (space group $C2/c$) and the ambient-temperature corundum (space group $R\bar{3}c$) structures are the energetically favored polymorphs (Figure 5). Neglecting vibrational effects, i.e., zero-point energies and contributions to the enthalpy and entropy, the bixbyite structure is about 9 kJ/mol per formula unit less stable than the M1 phase, supporting its classification as a metastable V_2O_3 polymorph. In order to further assess the thermodynamic stability at finite temperatures, the phonon density of states (pDOS) was calculated for V_2O_3 with the corundum and bixbyite structures. Both pDOS exhibit only positive values (Figure 5).

Thus, the new bixbyite polymorph does not spontaneously transform into a more stable polymorph. The absence of imaginary modes, which would appear as negative values in the

dx.doi.org/10.1021/ic200799n |Inorg. Chem. 2011, 50, 6762–6766

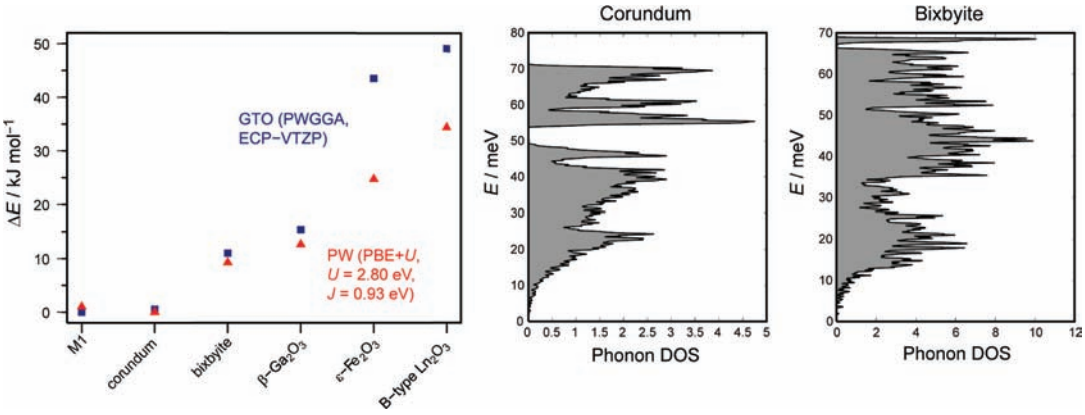

Figure 5. Energetic sequence of the six energetically lowest V_2O_3 polymorphs (left). Phonon density of states of the V_2O_3 corundum and bixbyite structure (right).

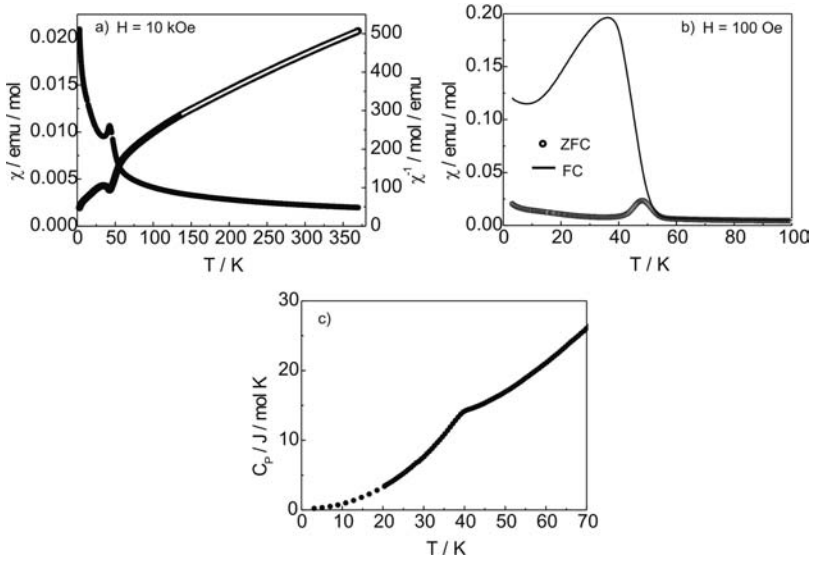

Figure 6. (a) $\chi(T)$ and $\chi^{-1}(T)$ measured at $H = 10$ kOe. The white line presents the fit of the modified Curie−Weiss law. (b) ZFC-FC measurement with $H = 100$ Oe. (c) Heat capacity measurement of V_2O_3.

phonon density of states and therefore indicate an inherent structural instability, confirms the metastable character of bixbyite-type V_2O_3.

Figure 6 displays the magnetic properties and heat capacity measurements of the new polymorph. A fitting between 130 and 300 K of $\chi^{-1}(T)$ with the modified Curie−Weiss law results in $\chi_0 = 4.7 \times 10^{-4}$ emu/mol, $\mu_{eff} = 1.68\,\mu_B$/V atom, and $\theta_P = -100$ K. χ_0 is $\chi_{dia} + \chi_{vv}$, where χ_{VV} is the paramagnetic van Vleck susceptibility and χ_{dia} is the diamagnetic core susceptibility. Assuming V_2O_3 to be an insulator, theoretical calculation of χ_0 reveals 3.43×10^{-4} emu/mol. Thus, a fixed χ_0 does not change the value of μ_{eff} significantly. However, the effective magnetic moment is much too small for V^{3+} (2.83 μ_B/V atom, high spin). In principle, the smaller value can be explained with either a strongly nonstoichiometric composition, which is not the case for this compound, with a metallic behavior due to a partially delocalization of the V spins or the presence of antiferromagnetic interactions well beyond the Néel temperature, thereby effectively reducing the moment derived from the Curie−Weiss plot. At around 50 K a magnetic ordering is visible. To identify the latter phenomena, ZFC-FC measurements at 100 Oe were performed and the antiferromagnetic transition was detected as well. The strong field dependence of that transition is indicative for a canted antiferromagnetic transition and/or spin-glass-like behavior. Heat capacity measurements at zero field show a broad transition with a maximum at around 40 K, establishing the field dependency and domains with slightly different stoichiometry.

The $M(H)$ measurement depicted in Figure 7 shows paramagnetic behavior at 300 K and a hysteresis at 40 K. With decreasing temperature the hysteresis is getting smaller and at 10 K $M(H)$ has an almost closed S-shaped course. However, the low-temperature behavior is not in the focus of this contribution. Detailed diffraction experiments together with investigations of the electrical and magnetic properties will be carried out, also with respect to the influence of the deviation from ideal V_2O_3 stoichiometry.

In air, fast oxidation of bixbyite-type V_2O_3 to V_2O_5 starts at around 523 K. Indicating a high reactivity even at ambient temperature, an oxidation to vanadium dioxide is observed after 3 weeks. In-situ powder X-ray diffraction measurements in argon atmosphere clearly show a phase transformation to thermodynamically stable

dx.doi.org/10.1021/ic200799n |Inorg. Chem. 2011, 50, 6762–6766

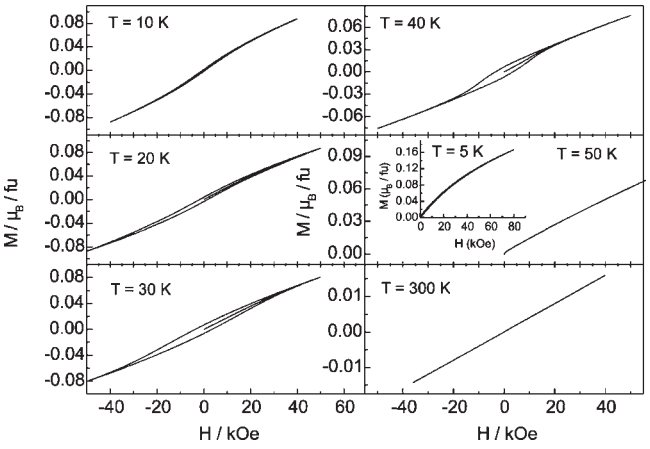

Figure 7. Magnetization M versus magnetic field H loops at different temperatures of V_2O_3.

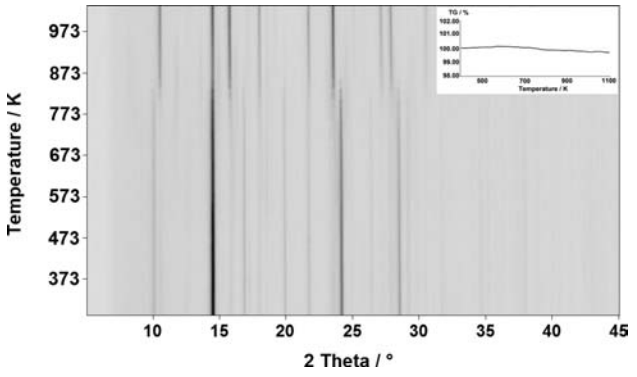

Figure 8. High-temperature X-ray powder diffraction patterns of bixbyite-type V_2O_3 in argon atmosphere. At ~823 K a phase transformation to corundum-type V_2O_3 is observed. The result of a TG measurement (10 vol % hydrogen in argon) is inserted.

corundum-type V_2O_3 at ~823 K (Figure 8), also indicating that bixbyite-type V_2O_3 should be considered as a metastable phase. Thermogravimetric analysis performed under 10 vol % hydrogen in argon resulted in no significant weight change, indicating how diminutive the deviation from ideal V_2O_3 stoichiometry is (Figure 8, inset). Simultaneous DTA measurements did not show any significant exo- or endothermic peak, although, as shown by analysis of the X-ray powder diagram of the cooled sample, the transformation to the corundum-type polymorph had taken place.

AUTHOR INFORMATION

Corresponding Author

*Fax: +49 (0) 30 314 79656. E-mail: lerch@chem.tu-berlin.de.

ACKNOWLEDGMENT

Financial support from the Deutsche Forschungsgemeinschaft (SPP 1415) is gratefully acknowledged.

REFERENCES

(1) Haber, J. *Catal. Today* **2009**, *142*, 100–113.
(2) Hess, C. *ChemPhysChem* **2009**, *10*, 319–326.
(3) Liu, P.; Lee, S.-H.; Cheong, H. M.; Tracy, C. E.; Pitts, J. R.; Smith, R. D. *J. Electrochem. Soc.* **2002**, *149*, H76–H80.
(4) Prosini, P. P.; Xia, Y.; Fujieda, T.; Vellone, R.; Shikano, M.; Sakai, T. *Electrochim. Acta* **2001**, *46*, 2623–2629.
(5) Muster, J.; Kini, G. J.; Park, J. G.; Burghard, M. *Adv. Mater.* **2000**, *12*, 420–424.
(6) Mott, N. F. *Metal-Insulator Transition*; Taylor and Francis Ltd.: London, 1974.
(7) Held, K.; Keller, G.; Eyert, V.; Vollhardt, D.; Anisimov, V. I. *Phys. Rev. Lett.* **2001**, *86*, 5345–5348.
(8) Finger, L. W.; Hazen, R. M. *J. Appl. Phys.* **1980**, *51*, 5362–5367.
(9) McWhan, D. B.; Remeika, J. B. *Phys. Rev. B* **1970**, *2*, 3734–3750.
(10) Dernier, P. D.; Marezio, M. *Phys. Rev.* **1970**, *2*, 3771–3776.
(11) Moon, R. M. *Phys. Rev. Lett.* **1970**, *25*, 527–529.
(12) Kraus, W.; Nolze, G. *Bundesanstalt für Materialprüfung (BAM), Berlin, Germany*, 2000.
(13) Roisnel, T.; Rodriguez-Carvajal, J. *Mater. Sci. Forum* **2001**, *378−381*, 118–123.
(14) Ressler, T. *J. Synchrotron Radiat.* **1998**, *5*, 118–122.
(15) Dovesi, R.; Orlando, R.; Civalleri, B.; Roetti, R.; Saunders, V. R.; Zicovich-Wilson, C. M. *Z. Kristallogr.* **2005**, *220*, 571–573.
(16) Dovesi, R.; Saunders, V. R.; Roetti, R.; Orlando, R.; Zicovich-Wilson, C. M.; Pascale, F.; Civalleri, B.; Doll, K.; Harrison, N. M.; Bush, I. J.; D'Arco, P.; Llunell, M. *CRYSTAL09* (CRYSTAL09 User's Manual); University of Torino: Torino, 2009.
(17) Kresse, G.; Furthmüller, J. *Comput. Mater. Sci.* **1996**, *6*, 15–50.
(18) Perdew, J. P.; Burke, K.; Ernzerhof, M. *Phys. Rev. Lett.* **1996**, *77*, 3865–3868.
(19) Perdew, J. P.; Chevary, J. A.; Vosko, S. H.; Jackson, K. A.; Pederson, M. R.; Singh, D. J.; Fiolhais, C. *Phys. Rev. B* **1992**, *46*, 6671–6687.
(20) Wolff, H.; Bredow, T.; Lerch, M.; Schilling, H.; Irran, E.; Stork, A.; Dronskowski, R. *J. Phys. Chem. A* **2006**, *111*, 2745–2749.
(21) Blöchl, P. E. *Phys. Rev. B* **1994**, *50*, 17953–17979.
(22) Liechtenstein, A. I.; Anisimov, V. I.; Zaanen, J. *Phys. Rev. B* **1995**, *52*, R5467–R5470.
(23) Ezhov, S. Y.; Anisimov, V. I.; Khomskii, D. I.; Sawatzky, G. A. *Phys. Rev. Lett.* **1999**, *83*, 4136–4139.
(24) Togo, A. Fropho, RWTH Aachen University, 2007−2008. Available at http://fropho.sourceforge.net.
(25) Stoffel, R.; Wessel, C.; Lumey, M.-W.; Dronskowski, R. *Angew. Chem., Int. Ed.* **2010**, *49*, 5242–5266.
(26) Dolg, M.; Wedig, U.; Stoll, H.; Preuss, H. *J. Chem. Phys.* **1987**, *86*, 866–872.
(27) Mackrodt, W. C.; Harrison, N. M.; Saunders, V. R.; Allan, N. L.; Towler, M. D.; Apra, E.; Dovesi, R. *Philos. Mag.* **1993**, *A 68*, 653–666.
(28) Martin, J. M. L.; Sundermann, A. *J. Chem. Phys.* **2001**, *114*, 3408–3420.
(29) Bredow, T.; Jug, K.; Evarestov, R. A. *Phys. Status Solidi B* **2006**, *243*, R10–R12.
(30) Nakhal, S.; Hermes, W.; Ressler, T.; Pöttgen, R.; Lerch, M. *Z. Naturforsch.* **2009**, *64b*, 281–286.
(31) Rundle, R. E.; Baenziger, N. C.; Wilson, A. S.; McDonald, R. A. *J. Am. Chem. Soc.* **1948**, *70*, 99–105.
(32) Masaki, N.; Tagawa, H. *J. Nucl. Mater.* **1975**, *57*, 187–192.
(33) Füglein, E.; Hock, R.; Lerch, M. *Z. Anorg. Allg. Chem.* **1997**, *623*, 304–308.